Shi, C., Lou, Y., Zhang, H., Zhao, Q., Geng, J., Wang, R., Fang, R., Liu, J. (2010): Seismic deformation of the Mw 8.0 Wenchuan earthquake from high-rate GPS observations. - Advances in Space Research, 46, 2, 228-235,

DOI: 10.1016/j.asr.2010.03.006

Estimating seismic displacement of the M_w 8.0 Wenchuan earthquake from high-rate GPS observations

C. Shi[a,b,*], Y. Lou[a], H. Zhang[a,b], Q. Zhao[a], J. Geng[c], R. Wang[d], R. Fang[a,b], J. Liu[a]

[a] *GNSS Research Center, Wuhan University, 129 Luoyu Road, Wuhan 430079, China*
[b] *State Key Laboratory of Information Engineering in Surveying, Mapping and Remote Sensing, 129 Luoyu Rd. Wuhan, 430079, China*
[c] *Institute of Engineering and Space Geodesy, the University of Nottingham, NG7 2RD, UK*
[d] *Helmholz Centre Potsdam, German Research Centre for Geosciences (GFZ), Telegrafenberg, 14473 Potsdam, Germany*

Abstract

High-rate GPS positioning has been recognized as a powerful tool in estimating epoch-wise station displacement which is particularly useful for seismology. In this study, station displacements during the 12 May 2008 M_w 8.0 Wenchuan earthquake are derived from the 1-Hz GPS data collected at a set of stations in China. The impacts of integer ambiguity resolution and station environment-dependent effects are investigated in order to yield more accurate results. The position accuracy of horizontal components of better than 1 cm suggests that GPS can sense the rapid position oscillation of about 2 cm in amplitude. Temporal and spatial analysis is applied to the surface displacement at station XANY and the characteristics of the movements due to Rayleigh and Love waves are detected and discussed. The comparison of GPS derived displacement with relevant synthetic data computed based on a recently published rapture model shows a reasonable agreement in waveform. The various differences in amplitude need further investigation and also imply that rapture inversion might be

*Corresponding author. Tel:+86-27-68778240; fax:+86-27-68778890

Email addresses: shi@whu.edu.cn (C. Shi), ydlou@whu.edu.cn (Y. Lou), hpzhang@whu.edu.cn (H. Zhang), zhaoql_gnss@hotmail.com (Q. Zhao), jhgeng1982@gmail.com (J. Geng), wang@gfz-potsdam.de (R. Wang), fangrongxin1006@163.com (R. Fang), jnliu@whu.edu.cn (J. Liu)

improved if GPS derived displacement is assimilated.

Keywords: High-rate GPS data, Wenchuan earthquake, seismic displacement

1. Introduction

In the earthquake studies, accelerometers, broadband seismometers, interferometric synthetic aperture radar (InSAR) and GPS are employed in order to resolve ground motions accurately over a range of frequencies and amplitudes which is very critical to the seismic rapture inversion. As is well known, each of them has its inherent strength and limitations. For example, accelerometers can capture the details of strong ground shaking near the source, but biased in the conversion from acceleration to displacement, whereas broadband seismometers are more sensible to ground motion but may saturate, and InSAR has a coarse temporal resolution of more than tens of days.

Since decades, GPS plays an important role in the long-term crustal deformation monitoring and estimation of the co-seismic offsets. As GPS precision and methodologies have improved, high-rate GPS data have been used in monitoring transient and seismic deformation (Bock et al. , 2000; Larson et al., 2003; Kouba, 2003; Bock and Prawirodirdjo, 2004; Irwan et al., 2004). Several studies have confirmed that the displacement derived from high-rate GPS data coincides with those from the seismic sensors and the simulated platform shaking at the level of 6 mm (Bock and Prawirodirdjo, 2004; Elósegui et al., 2006; Emore et al., 2007).

The high-rate GPS data can capture the rapid co-seismic ground displacements over a range of frequencies and amplitudes that are in some sense wider than the seismic sensors can do. For example, Wang et al. (2007) demonstrated that 1-Hz GPS data can sufficiently describe the crustal movement of which the frequency is over 0.5 Hz caused by earthquakes and Bock and Prawirodirdjo (2004) demonstrated its capability of detecting arbitrarily large dynamic ground motions and sensing seismic surface waves from several hundreds or even thousands of kilometers away. More important is that the derive displacements have been already used into fault slip detections and rapture inversions (Chen et al., 2004; Langbein and Bock , 2004; Miyazaki et al., 2004; Blewitt et al., 2006; Sobolev et al., 2007; Hoechner et al., 2008).

The 12 May 2008 M_w 8.0 Wenchuan earthquake devastated cities and claimed at least 69000 lives in Sichuan Province, China. Due to the very complicated geological structures in the region, the earthquake process is still under investigation. More crucial is that the earthquake may trigger or hasten additional earthquakes (Toda et al., 2008).

Due to the aforementioned advantages of GPS high-rate data and the failures of a number of seismic sensors during the earthquake, GPS-derived displacements may provide additional and more important information for the further in-depth studies on the rupture process. In this study, we estimate the displacements from the 1-Hz GPS data collected at a set of stations within China around the earthquake time using the data processing strategies with recent improvements to achieve the best results. The displacements are analyzed and interpreted in both the frequency and spatial domain for a better understanding of the contribution of Love and Rayleigh waves to the station movements. The synthetic displacements at the relevant GPS stations are computed as well from a recently published rapture model. In general, the observed seismic displacements agree well in waveform with the synthetics. The remaining disagreement in amplitude might be important for a more precise rapture inversion with the GPS derived displacements.

2. GPS data processing

To date, there are two approaches in estimating epoch-wise station positions epoch-by-epoch with high-rate GPS data: network solution (Bock and

Prawirodirdjo, 2004; Larson, 2009)and Precise Point Positioning (PPP) technique (Larson et al., 2003; Kouba, 2003; Geng et al., 2010).

In the former approach at least one station must be fixed or tightly constrained to its known values, although it is normally also displaced by the seismic motions. Therefore, the displacements estimated for the other stations are biased by the displacement of the fixed station. In order to obtain displacement with respect to a reference frame, stations which are not affected by the earthquake should be included as reference stations into the data processing. As the position accuracy in the relative positioning degrades usually along with the baseline length, the inter-station distance is limited to several tens to hundreds kilometers as in the published studies (Bock and Prawirodirdjo, 2004; Larson, 2009).

In the PPP approach where satellite clocks and orbits are fixed to pre-estimated precise values, for example, the International GNSS services (IGS) final products, and the coordinates can be estimated station by station in the reference frame defined by the orbits and clocks. The ambiguity-fixing can also be performed in network mode or single point mode (Ge et al., 2008; Geng et al., 2010) which improves the horizontal accuracy significantly. However, orbit and clock errors may propagate directly into the estimated position, as they are fixed in the estimation.

As the inter-station distances range from several hundreds to thousands kilometers (see Figure 1), the PPP approach will be employed in this study and the results are investigated carefully.

2.1. Data set

Among the hundreds of GPS stations in China, most of the stations that record 1-Hz GPS data are the regional CORS (Continuous Operational Reference Station) stations. They are set up for providing precise positioning services over a region, for example, a large city or a province. The CORS systems are now established only in large cities and in some of the developed provinces and not all the data are accessible due to the various policy of data management. We have collected the data at some stations of the CORS networks in Chongqin, Xi'an , Kunming, Wuhan and Shanghai which are about 350 km, 650 km, 1000 km, 1000 km and 1600 km away from the epicenter, respectively. Figure 1 shows the location of the cities and the earthquake epicenter. The station names are listed below the city names.

2.2. Processing strategies

The data are processed with the PANDA (Position And Navigation system Data Analyst) software which is developed at the GNSS Research Center at Wuhan University as a multi-functional tools for GNSS research and applications (Liu and Ge, 2003; Shi et al., 2008). Its performances in precise static and kinematic positioning are demonstrated by Ge et al. (2008) and Geng et al. (2010).

Data around the earthquake time, from 0:00 to 12:00 UTC on 12 May 2008, are processed in PPP mode, whereas the ambiguity-fixing is performed in network mode. The observation models in IERS (International Earth Rotation Services) conventions 2003 and recommended by IGS are implemented in the software and used in the data processing, such as tide displacement, absolute antenna phase center correction etc. Satellite orbits, clocks and Earth rotation parameters are fixed to the CODE (Center for Orbit Determination in Europe) final products. Station coordinates and receiver clocks are estimated epoch-by-epoch. The tropospheric delays are corrected using the zenith total delay (ZTD) from Saastamoinen model with the Vienna mapping function (Boehm et al., 2006). The residual ZTD is parameterized as a random walk process with a priori constraint of 10 cm to its initial state and $2cm/\sqrt{hour}$ power density. Zero-differenced ionosphere-free observations with elevation above $7°$ are used in the estimation with elevation-dependent weight. The least-squares estimator with an efficient approach of removal and recovery of station coordinates and ambiguity parameters is employed in order to speed up the data processing (Ge et al., 2006).

Data from the days before the earthquake are also processed in order to evaluate the effect of the multi-path and other station environment-dependent error sources. Sidereal filter is applied on the coordinate time series to improve the GPS derived displacement.

3. Results and Discussion

The epoch-wise station coordinates estimated from the days before the earthquake using PPP approach are compared with their static solutions with the same data. The RMS of their differences is about 1.0 cm, 1.5 cm and 2.8 cm in the north, east and up components. The large RMS in the vertical component is because the height estimates are strongly correlated with the zenith tropospheric delays and are very sensitive to the tropospheric modeling and parameterization (Kouba, 2003).

The horizontal components are improved by ambiguity-fixing to better than 0.8 cm and 0.9 cm which is similar to the accuracy achieved by Geng et al (2010). Figure 2 shows an example for the improvement of ambiguity-fixing for station KMKC in Kunming city. The differences in the east and north directions between epoch-wise and static estimates are reduced after ambiguity-fixing from 3.2 cm to 1.2 cm and 1.1 cm to 0.9 cm , respectively. A larger draft in the east component disappears in the fixed solution.

Figure 3 shows the east component from the two days before the earthquake and the earthquake day of the station KMKC in Kunming city. The similar patterns repeated on daily base shown up in the time series imply that there are station dependent error sources, such as multi-path effects and performance of the receivers, which can be removed based on the results from previous days by means of sidereal filter (Larson et al 2007). Figure 3, also shows the significant improvement of sidereal filter on the time series,which reduces the RMS from 1.3 cm to 0.7 cm.

3.1. Characteristics of seismic waveforms

Seismic waveform data can provide an insight on the dynamic rupture process of the earthquake. Figure 4 shows the horizontal displacement starting at the earthquake epoch and lasting for 10 minutes at stations SHQP, HUPI, CHGO, XANY, and BISH which are located at different cities. They are arranged in terms of their distances to the epicenter from the top to the bottom panels. This is also reflected in the different response times of the station movements.

From the time series, there are still systematic fluctuations of 1-2 centimeters which might be caused by errors in satellite clocks and orbits fixed in the processing and by remaining station environment errors. However, the fluctuations are rather slow compared to the rapid position oscillations deduced by the earthquake. Therefore, the displacement of about 2 cm in amplitude at SHQP station in Shanghai which is about 1600 km from the epicenter can still be detected easily.

Comparing the displacements at the five stations, we can indicate the following three prominent characteristics. First of all, the amplitude of the displacement at the station BISH which is the nearest station to the epicenter is relatively small of only 5 cm, whereas the station XANY shows the largest amplitude of up to 15 cm. Then, the co-seismic displacement at station XANY, lasting for up to 150 s, shows much more complicated information particularly at high frequency than that of other stations. Finally, once the surface seismic wave arrived, station CHGO moved west-southward whilst all other stations west-northward. As shown in the plots, the north component of station CHGO decreases while those of the other stations increase.

All these issues may reflect the earthquake source dynamics. The fault of the

Wenchuan earthquake strikes from southwest to northeast and dips to northwest. The epicenter is located about the southwest end of the fault. The focal mechanism is dominated by the thrust fault but with a significant right-lateral strike-slip component in the northeast segment (Wang et al. 2008). The station XANY is just located in the direction of the rupture propagation and thus shows large amplitude with high-frequency content, resulted from the interference effect.

In order to better understand the observed seismic displacement waveforms, we calculated the synthetic seismograms at all the relevant stations (Fig. 5) using the reflectivity code by Wang (1999). The earthquake rupture model is adopted from Wang et al. (2008). In general, the observed GPS seismograms agree well with the synthetic results. Especially, the polarization of the start phase observed at most stations is verified by the seismic model. Also the large amplitude with high-frequency content at the station XANY is reasonable. On the other hand, however, the coda wave shown by the synthetic seismogram at XANY is considerably shorter than observed. A possible reason may be the site effect at this station that is not included in the synthetic data. In addition, the observed displacement amplitude at the station BISH is much smaller than expected.

3.2. Surface waves observed at the station XANY

We further analyzed the waveform of the co-seismic displacement at station XANY. Fortunately, this station is located in the direction of the rupture propagation, thus showing the largest directivity effect. In fact, the azimuth of the SW and NE end of the fault to the station is about 230° and 240°, respectively, very close to the fault strike of 229°. Therefore, we projected the two horizontal components of the synthetic and observed seismograms to the radial ($N50^{\circ}E$) and tangential ($N140^{\circ}E$) directions (upper panel of Fig. 6).

It is obvious that the tangential component is significantly larger than the radial component, consistent with the dominant thrust mechanism of the earthquake. A good agreement can be seen between the synthetic and observed S wave signals with a characteristic duration of 35 sec that is about three times shorter than the rupture process of about 100 sec due to the Doppler effect. Whereas the arrival time of the S wave agrees well with that shown in the synthetic seismograms, the Love and Rayleigh waves arrive significantly later than expected theoretically, implying a lower crustal S wave velocity than that used in the seismic model.

The surface waves are characterized by two dominant frequencies, around 0.05 Hz (20 sec in period) and 0.15 Hz (7 sec). The lower frequency surface waves appear mainly in the head part of the seismograms (200. - 240. sec). This time window generally includes regional surface waves, as it can also be confirmed by the synthetic data. The higher frequency is given by the coda wave (lower right panel of Fig. 6) that is missing in the synthetic data. A possible explanation is the local effect based on several indications: (1) small head amplitude, (2) narrower frequency band and (3) less consistent polarization than the regional surface waves. Such coda wave is usually generated in local sediment basin.

4. Conclusions

We have processed the 1-Hz GPS data at several stations in China during the Wenchuan earthquake using PPP approach. Impacts of ambiguity-fixing and station environment on the derived station displacements are investigated. The RMS of better than 1 cm in the horizontal component of the displacements confirms that the rapid position oscillations caused by the earthquake of about 2 cm in amplitude can be detected reliably.

We have also compared the estimated station displacements with the synthetic data calculated from a recent published rapture model. In general, they agree with each other, especially, in the polarization of the start phase. The largest surface waves were observed at the station XANY that is just located in the direction parallel with the rupture propagation. Both Rayleigh and Love wave signals have two dominant periods at about 20 sec and 7 sec. The shorter period is missing in the synthetic data and is possibly related to the local shallow sediment structure.

The various differences between the observed GPS seismograms and the seismic model need further investigation and may also be a possibility that the rapture inversion can be still improved by assimilating GPS derived displacement.

Acknowledgement

This work is supported by China 973 project (2006CB701301) and 863 program (2007AA120603). We are grateful to Dr Shuanggeng Jin for his helpful suggestions, which improved the manuscript greatly.

References

Blewitt, G., C. Kreemer, W.C. Hammond, H.-P. Plag, S. Stein, and E. Okal (2006), Rapid determination of earthquake magnitude using GPS for tsunami warning systems, Geophys. Res. Lett., 33, L11309, doi:10.1029/2006GL026145.

Bock Y., R. M. Nikolaidis, P. J. de Jonge, and M. Bevis (2000), Instantaneous geodetic positioning at medium distances with the Global Positioning System, J. Geophys. Res., 105, 28223-28253

Bock, Y. and L. Prawirodirdjo(2004), Detection of arbitrarily large dynamic ground motions with a dense high-rate GPS networks, Geophys. Res. Lett., 31, L06604, doi:10.1029/2003GL019150

Boehm, J., B. Werl, and H. Schuh (2006), Troposphere mapping functions for GPS and very long baseline interferometry from European Centre for Medium-Range Weather Forecasts operational analysis data, J. Geophys. Res., 111, B02406, doi:10.1029/2005JB003629

Chen J., K. M. Larson, Y. Tan, K. W. Hudnut, and K. Choi (2004), Slip history of the 2003 San Simeon earthquake constrained by combining 1-Hz GPS, strong motion, and teleseismic data, Geophys. Res. Lett., 31, L17608, doi: 10.1029/2004GL020448

Elósegui, P., J. L. Davis, D. Oberlander, R. Baena, and G. Ekström (2006), Accuracy of high-rate GPS for seismology, Geophys. Res. Lett., 33, L11308, doi:10.1029/2006GL026065

Emore, G. L., J. S. Haase, K. Choi, K. M. Larson, and A. Yamagiwa(2007), Recovering Seismic Displacements through Combined Use of 1-Hz GPS and Strong-Motion Accelerometers, Bull.Seismol.Soc.Am., 97(2), 357-378

Ge M. G. Gendt, G. Dick, F. P. Zhang, and M. Rothacher (2006), A new data processing strategy for huge GNSS global networks, J.Geod., Vol.80, pp199-203, doi 10.1007/s00190-006-044-x.

Ge M., G. Gendt, M. Rothacher, C. Shi, & J. Liu, Resolution of GPS carrier-phase ambiguities in Precise Point Positioning (PPP) with daily observations, J.Geod., 82, 389-399, 2008.

Geng, J., F.N. Teferle, X. Meng, A.H. Dodson (2010) Kinematic precise point positioning at remote marine platforms. GPS Solut.online

Hoechner A., A. Y. Babeyko, S. V. Sobolev (2008), Enhanced GPS inversion technique applied to the 2004 Sumatra earthquake and tsunami, Geophys. Res. Lett., 35, L08310, doi: 10.1029/ 2007GL033133

Irwan, M., F. Kimata, K. Hirahara, T. Sagiya, and A. Yamagiwa (2004), Measuring ground deformations with 1-Hz GPS data: the 2003 Tokachi-oki earthquake (preliminary report), Earth Planets Space, 56, 389-393

Jin, S.G., P.H. Park, and W.Zhu(2007), Micro-plate tectionics and kinematics in Northeast Asia inferred from a dense set of GPS observations, Earth and Planetary Science Letters, 257, 486-496, doi: 10.1016/j.epsl.2007.03.011

Kouba J. (2003), Measuring seismic waves induced by large earthquake with GPS, Stud. Geophys. Geod., 47, 741-755

Larson, K. M., P. Bodin, and J. Gomberg (2003), Using 1-Hz GPS data to measure deformations caused by the Denali fault earthquake, Science, 300(5624), 1421-1424

Larson, K. M., A. Bilich, and P. Axelrad (2007), Improving the precision of high-rate GPS, J. Geophys. Res., 112, B05422, doi:10.1029/2006JB004367.

Larson K. M.(2009), GPS seismology, J. Geod., 83:227-233, doi 10.1007/s00190-008-0233-x

Langbein J. and Y. Bock (2004), High-rate real-time GPS network at Parkfield: Utility for detecting fault slip and seismic displacements, Geophys. Res. Lett., 31, L15S20, doi:10.1029/2003GL019408

Liu J. and M. Ge(2003) PANDA software and its preliminary result of positioning and orbit determination. J Nat Sci Wuhan Univ 8(2B):603-609. doi:10.1007/BF02899825

Liu J., Z.Zhang, L.Wen et al.(2009). Co-seismic ruptures of the 12 May, 2008, Mw 8.0 Wenchuan earthquake, Sichuan: Ew crustal shortening on oblique, prallel thrusts along the eastern edge of Tibet. Earth and Planetary Science Letters, 286, 355-370.

Miyazaki S., K. M. Larson, K. Choi, K. Hikima, K. Koketsu, P. Bodin, J. Haase, G. Emore, and A. Yamagiwa (2004), Modeling the rupture process of the 2003 september 25 Tokachi-Oki (Hokkaido) earthquake using 1-Hz GPS data, Geophys. Res. Lett., 31, L21603, doi: 10.1029/ 2004GL021457

Shi C, Q. Zhao, J. Geng, Y. Lou, M. Ge, and J. Liu (2008), Recent development of PANDA software in GNSS data processing. In: Proceedings of the Society of Photographic instrumentation Engineers, 7285, 72851S, doi: 10.1117/12.816261

Sobolev, S. V., A. Y. Babeyko, R. Wang, A. Hoechner, R. Galas (2007), Tsunami early warning using GPS-Shield arrays, J. Geophys. Res., 112, B08415, doi: 10.1029/2006JB004640.

Toda, S., J. Lin, M. Meghraoui, and R. S. Stein (2008), 12 May 2008 M_w= 7.9 Wenchuan, China, earthquake calculated to increase failure stress and seismicity rate on three major fault systems, Geophys. Res. Lett., 35, L17305, doi:10.1029/2008GL034903.

Wang G., D. M. Boore, G. Tang, and X. Zhou (2007), Comparisons of Ground Motions from Colocated and Closely Spaced One-Sample-per-Second Global Positioning System and Accelerograph Recordings of the 2003 M6.5 San Simeon, California Earthquake in the Parkfield Region, Bulletin of the Seismological Society of America, Vol. 97, No. 1B, pp76-90, doi:10.1785/0120060053.

Wang, R. (1999), A simple orthonormalization method for stable and efficient computation of Green's functions, Bull. Seismol. Soc. Am., 89, 733- 741.

Wang W. L. F. Zhao, J. Li, and Z X. Yao (2008). Rupture process of the Ms 8.0 Wenchuan earthquake of Sichuan, China. Chin.J.Geophysics, 51(5):1405-1410 (in Chinese).

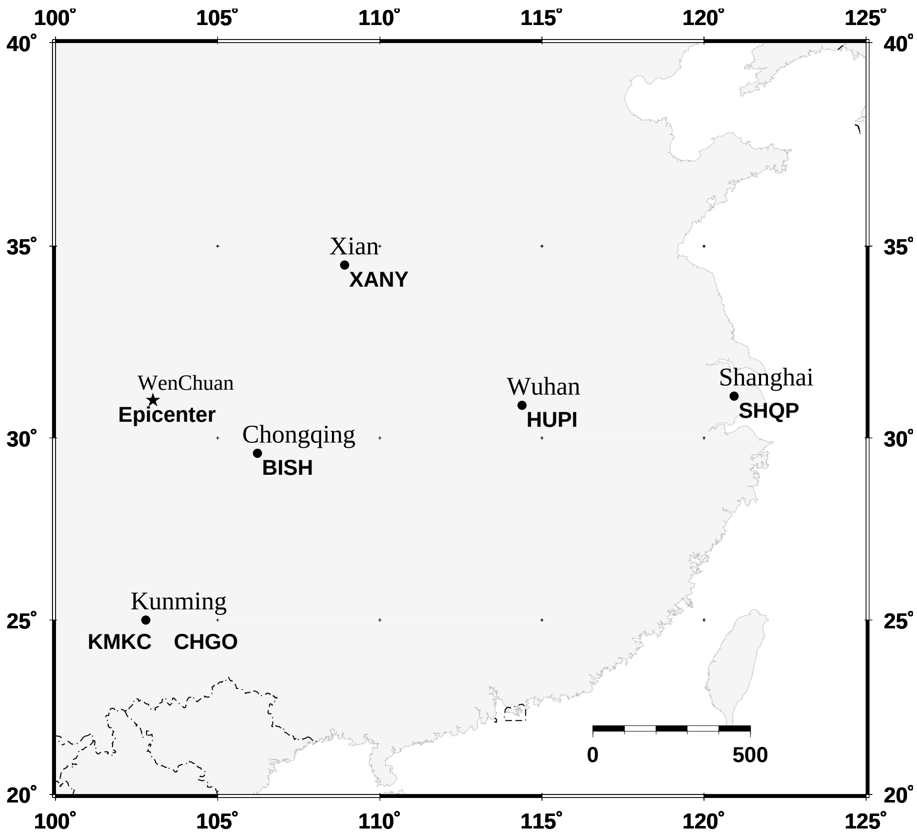

Figure 1: Distribution of the 1-Hz GPS stations during the M_w 8.0 Wenchuan earthquake in 2008. The stations are mainly from the regional CORS networks from the relevant cities. The station names are listed under the city names.

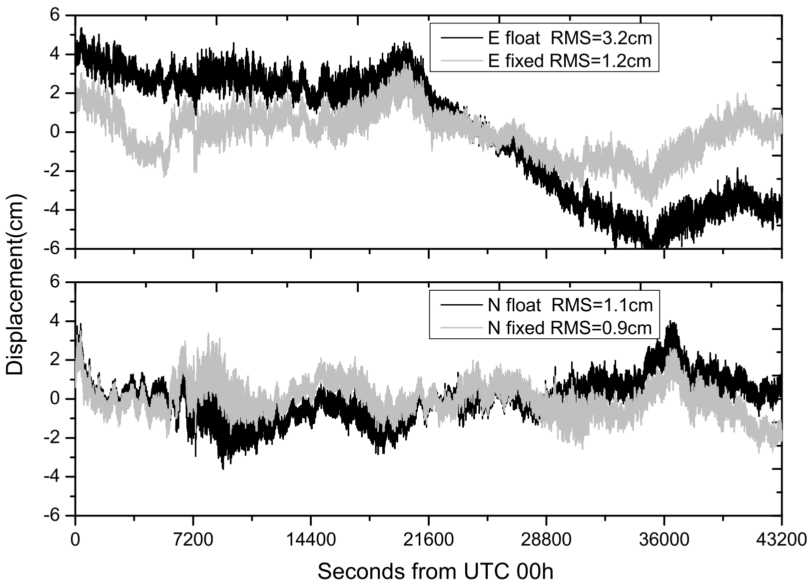

Figure 2: Improvement of ambiguity-fixing on the estimated coordinates of station KMKC. The differences in east and north directions between epoch-wise and static estimates are reduced with ambiguity-fixing from 3.2 cm, 1.2 cm to 1.1 cm and 0.9 cm , respectively.

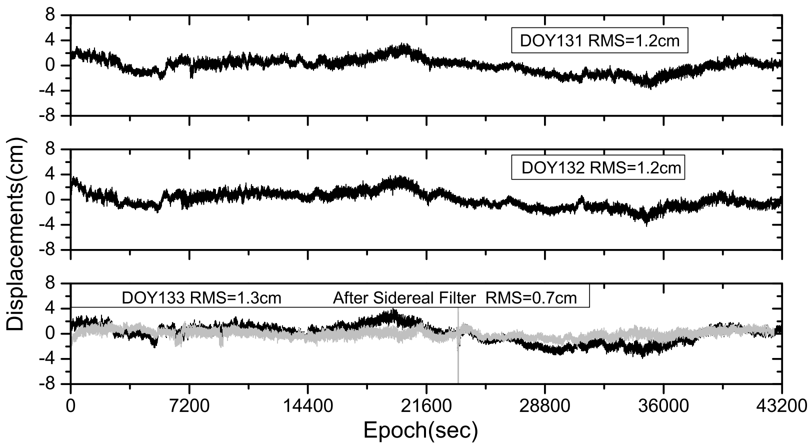

Figure 3: Multi-path impact on epoch-wise estimated coordinates for station KMKC. The top and the middle panels show the differences in east direction of the two previous days. The buttom panel shows the differences on the earthquake day and the differences after removing the systematic error using sidereal filtering where the rms is improved from 1.3 cm to 0.7 cm.

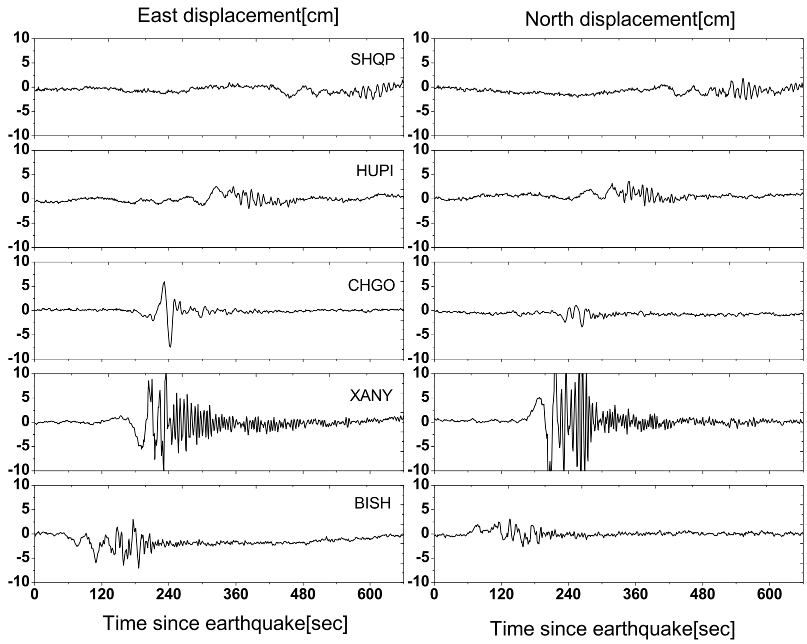

Figure 4: Displacement in east and north directions for stations SHQP, HUPI, CHGO, XANY, and BISH since the earthquake time. They are in the decreasing order of their distances to the epicenter from top to button.

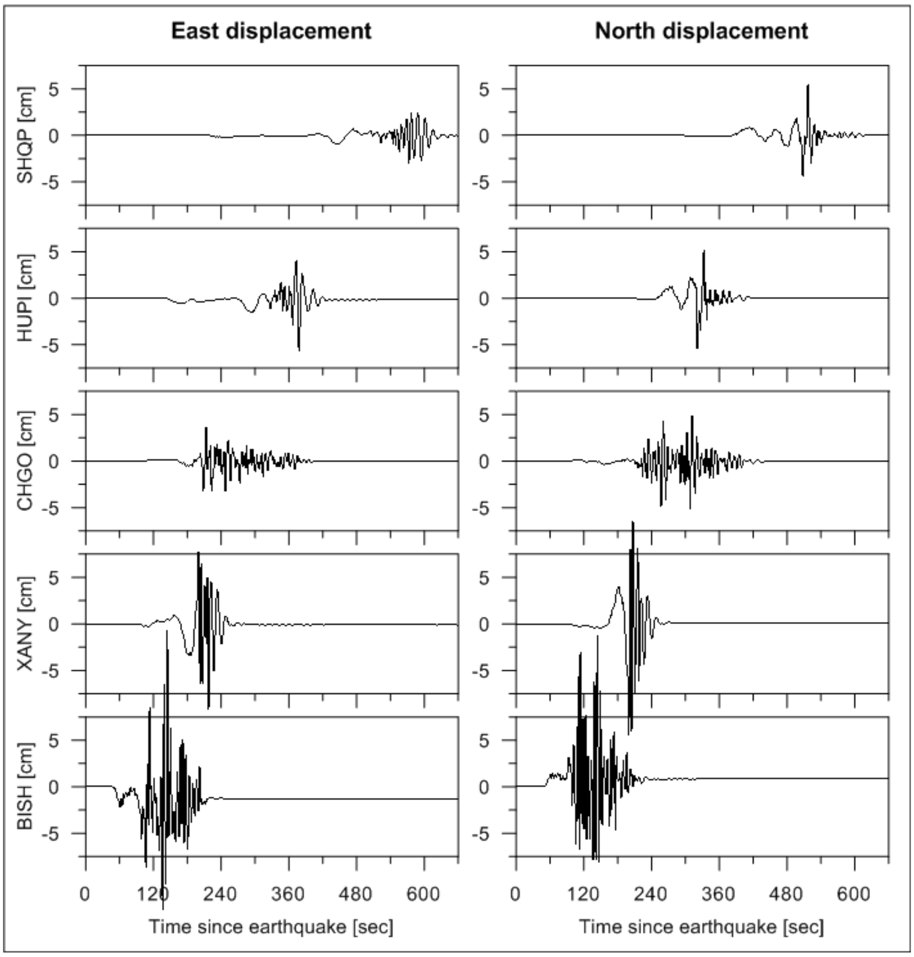

Figure 5: The synthetic seismograms at the stations SHQP, HUPI, CHGO, XANY, and BISH using the reflectivity code by Wang (1999). The earthquake rupture model is adopted from Wang et al. (2008).

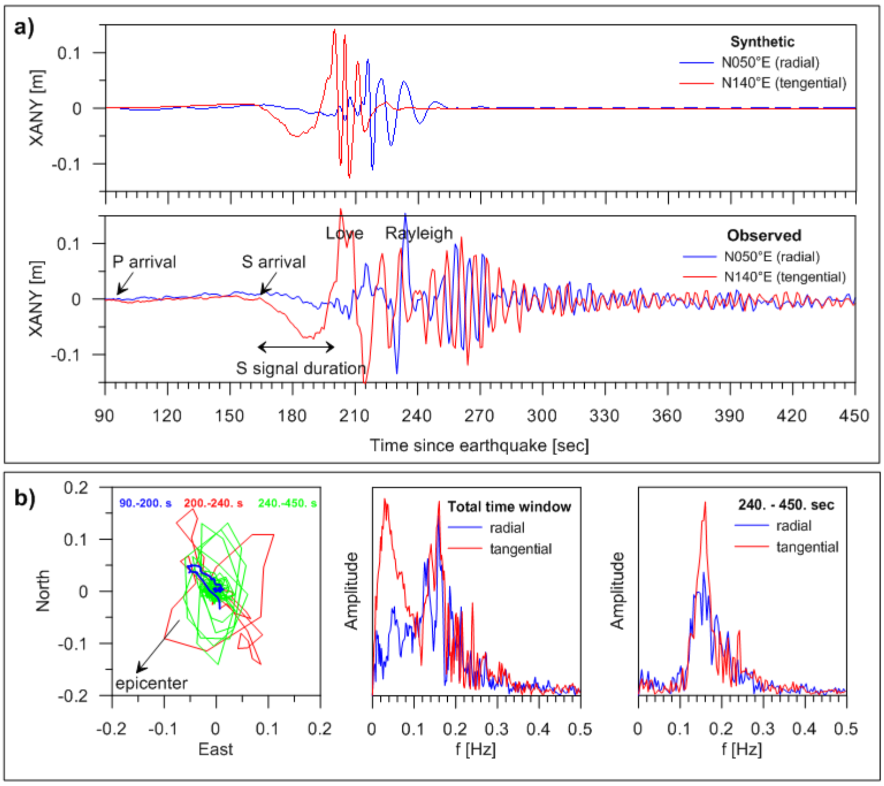

Figure 6: Co-seismic displacement at the station XANY, projected in radial and tangential directions to the epicenter. The upper panel (a)shows the comparison with the synthetic seismograms and (b) the polarization and Fourier spectrum at selected time intervals.